NeuroImage: Clinical 23 (2019) 101924

Contents lists available at ScienceDirect

NeuroImage: Clinical

journal homepage: www.elsevier.com/locate/ynicl

Reduced brainstem functional connectivity in patients with peripheral autonomic failure

Jacquie Baker[a,b,*], Kurt Kimpinski[a,c]

[a] School of Kinesiology, Western University, London, Ontario, Canada
[b] Department of Clinical Neurological Sciences, University Hospital, London Health Sciences Centre, London, Ontario, Canada
[c] Schulich School of Medicine & Dentistry, Western University, London, Ontario, Canada

ARTICLE INFO

Keywords:
Brainstem
Functional connectivity
Autonomic failure
Neurogenic orthostatic hypotension
Central autonomic network

ABSTRACT

Autonomic homeostasis is dependent upon several brainstem nuclei, as well as several cortical and subcortical structures. Together, these sites make up, in part, the central autonomic network. Neurogenic orthostatic hypotension (NOH) is a cardinal feature of autonomic failure that occurs due to a failure to increase sympathetic efferent activity in response to postural changes. Therefore, the purpose of the current study was to investigate brainstem functional connectivity in NOH patients with peripheral autonomic lesions resulting in autonomic failure.

Fifteen controls (63 ± 13 years) and fifteen Neurogenic Orthostatic Hypotension patients (67 ± 6 years; $p = .2$) with peripheral autonomic dysfunction completed 5-min of rest and three Valsalva maneuvers during a functional brain scan. Functional connectivity from the brainstem to cortical and subcortical structures were contrasted between patients and controls.

At rest controls had significantly greater brainstem connectivity to the anterior cingulate cortex (T-value: 4.29), left anterior insula (T-value:3.31), left putamen (T-value:3.31) and bilateral thalamus (T_{RIGHT}-value: 3.83; T_{LEFT}-value:4.25) (p-FDR < 0.005). During Valsalva, controls showed significantly more connectivity between the brainstem and both the left anterior (cerebellum 4/5) and bilateral posterior cerebellum (cerebellar 9 and left cerebellar 6). Other cerebellar regions included brainstem-to-vermis. Other brainstem-to-cortical and subcortical regions included: bilateral putamen, posterior cingulate cortex (PCC), amygdala and medial prefrontal cortex. There was a significant negative correlation between the brainstem-cerebellar connectivity and severity of autonomic dysfunction ($p < .01$). During recovery phase of the Valsalva, controls had greater brainstem connectivity to the left thalamus (T-value:4.17); PCC (T-value:3.32); right putamen (T-value:3.28); right paracingulate gyrus (T-value:3.25) and left posterior cerebellum (C9) (T-value:3.21) (p-FDR < 0.05). The effect sizes for each brainstem connectivity during Valsalva and recovery ranged from moderate to strong.

Patients with autonomic failure show reduced coupling between the brainstem and regions of the central autonomic network, including the cerebellum, insula, thalamus and cingulate cortices. Connectivity was associated with autonomic impairment. These findings may suggest impaired brainstem connectivity in patients with autonomic failure.

1. Introduction

Neurogenic Orthostatic Hypotension (NOH) is a cardinal feature of autonomic failure. NOH is clinically defined as a sustained reduction in blood pressure ≥ 30 mmHg during an orthostatic challenge such as standing from a lying or seated position or during head-up tilt performed at a minimum 60° angle from the horizontal (Gibbons et al., 2017). NOH occurs due to a failure of the sympathetic reflexes that would normally counteract blood pressure perturbations through reflexive tachycardia and vasoconstriction. Generally speaking, classifications of NOH are made based on where failure of the sympathetic efferent signaling pathway occurs i.e. before or after the autonomic ganglia. For example, in clinical populations such as Parkinson's Disease (PD) with autonomic failure, Pure Autonomic Failure (PAF) and diabetic autonomic neuropathies, the lesion site is considered to be post-ganglionic.

Autonomic homeostasis is dependent upon several brainstem nuclei, including the nucleus tractus solitarius (NTS) and rostral and caudal

* Corresponding author at: Rm. B7-140, University Hospital, London Health Sciences Centre, 339 Windermere Road, London, Ontario N6A 5A5, Canada.
E-mail address: jbaker62@alumni.uwo.ca (J. Baker).

https://doi.org/10.1016/j.nicl.2019.101924
Received 12 April 2019; Received in revised form 31 May 2019; Accepted 30 June 2019
Available online 02 July 2019

portions of the ventrolateral medulla. For example, the NTS receives afferent input and through a cascade of excitatory and inhibitory signaling makes beat-to-beat adjustments to efferent autonomic outflow. Moreover, various autonomic brainstem nuclei have been shown to project to both cortical and subcortical regions and have also been shown to receive input from higher cortical structures (Castle et al., 2005; Saper, 1982; Verberne et al., 1997). Through advancements in neuroimaging, several cortical and subcortical structures including the insula, hippocampus, cerebellum, thalamus and cingulate cortices, have been well established as components of the central autonomic network (CAN) (Benarroch, 1993; Oppenheimer et al., 1992; Shoemaker et al., 2015; Verberne and Owens, 1998). Importantly, studies have not only tested different modalities, but have also correlated brain activation patterns to hemodynamic responses and direct measures of sympathetic activity. Together, these studies have identified structures of the CAN that contribute specifically to sympathetic and parasympathetic regulation.

Based on the aforementioned pre- versus post-ganglionic classification of autonomic failure, it could be thought that brainstem nuclei and structures of the CAN would remain functionally intact. However, our laboratory recently demonstrated that despite post-ganglionic pathology, NOH patients show evidence of reduced activation in regions of the CAN during autonomic maneuvers (Baker et al., 2019; Baker et al., 2018).

Despite the fact that the brainstem is the main region for central integration of baro- and chemoreceptor afferents, brainstem-to-brain connectomes have not been fully investigated. Specifically, the evaluation of functional connectivity between the brainstem and regions of the CAN in individuals with autonomic failure has yet to be studied.

Therefore, our aim was to investigate whether functional connectivity from the brainstem to cortical and subcortical structures differs in patients with NOH secondary to autonomic failure as compared to their healthy counterparts.

2. Methods

2.1. Studied population

The current study was comprised of fifteen healthy, age-matched controls (61 ± 14 years; females: 8) and 15 patients diagnosed with NOH (67 ± 6 years; females: 6; $p = .12$). Our NOH population consisted of patients with evidence of peripheral autonomic denervation only (PAF, $n = 4$; PD with autonomic failure, $n = 6$; idiopathic NOH, $n = 5$). All patients underwent a standard head-up tilt (HUT) test and met the clinical criteria for NOH. Hemodynamic data at rest and in response to HUT are presented in Table 1. As an additional assessment of autonomic dysfunction, all patients demonstrated absent adrenergic phases (late phase II and phase IV) in response to the Valsalva maneuver and cardiovagal impairment evidenced by a reduced Valsalva ratio (1.21 ± 0.17). These data were replicated during the MRI session where patients had an average Valsalva ratio of 1.22 ± 0.11. Furthermore, to provide clinical evidence of post-ganglionic impairment, all patients underwent quantitative sudomotor axon reflex testing (QSART) from four standard sites (forearm, proximal leg, distal leg and foot). Sudomotor dysfunction was scored as follows: 1 = reduced sweat response at a single site, 2 = absent response at a single site, 3 = absent response at 2 or more sites. The composite autonomic scoring scale (CASS) was used to quantify the severity and distribution of autonomic failure across three domains: sudomotor (0–3), cardiovagal (0–3) and adrenergic (0–4) (Low, 1993). On average patients scored a 2/3, 2/3 and 4/4, respectively, resulting in a total CASS of 8/10 indicative of severe and widespread autonomic dysfunction. Patients reported an average symptom duration of 7 ± 5 years, and PD + autonomic failure patients had an average score of 2.7 (range: 2–4) on the Hoehn and Yarh scale.

Patients with neurodegenerative disorders related to a central autonomic pathology (i.e. Multiple System Atrophy) were excluded from the present study to eliminate any potentially confounding variables associated with such central pathologies (i.e. brain atrophy). Moreover, NOH patients were excluded if there was evidence of any peripheral nerve injury unrelated to their diagnosis of autonomic dysfunction including diabetic neuropathies in any form. In the current study, Pure autonomic failure (PAF) was defined as a sporadic disorder characterized by orthostatic hypotension along with more widespread autonomic failure, including sympathetic and parasympathetic dysfunction. In addition, PAF patients showed no clear identifiable underlying cause, no other neurological features present and no features to suggest central involvement. PAF patients had maintained a purely peripheral autonomic failure without any evidence of other pathology for an extended period of time. In contrast, a diagnosis of idiopathic NOH was given if, again, there was evidence of orthostatic hypotension, along with gastrointestinal issues or other questionable phenomenon such as olfactory impairment, but not meeting criteria for other alpha-synucleinopathies. As such, with these patients a clearer, more specific diagnosis may become more apparent with time. A neurologist (KK) confirmed all testing and made the final diagnoses.

All healthy participants were examined to confirm the absence of any neurological conditions including any autonomic dysfunction. Additional exclusion criteria including the following categories: i) pregnant or lactating females, ii) clinically significant coronary artery disease, iii) concomitant therapy with anticholinergic, alpha- and beta-adrenergic antagonists or other medications which could interfere with autonomic functioning, and iv) failure of other organ systems or systemic illness that could affect autonomic function or participants' ability to cooperate.

All laboratory data were collected in the Autonomic Disorders Laboratory at University Hospital, London, Ontario. All functional imaging data were collected at Robart's Research Institute Centre for Functional and Metabolic Imaging at The University of Western Ontario. Ethical approval was obtained from the Health Science Research Ethics Board at Western University, and informed consent was obtained from all participants prior to testing.

2.2. Neuroimaging data acquisition

All imaging data were collected using a whole body 3 T imaging system with a 32-channel head coil (Magnetom Primsa, Siemens Medical Solutions, Erlangen, Germany). At the beginning of the scanning session, a 3D MPRAGE sequence was used to acquire a high-resolution T1-weighted structural (sagittal, matrix 256 × 240mm, voxel

Table 1
Patient heart rate and blood pressure data at rest and in response to head-up tilt.

	Resting HR (bpm)	ΔHR (bpm)	Resting SBP (mmHg)	ΔSBP (mmHg)
25% Percentile (Q1)	55.8	1	92	−60.8
Median	67.4	6.7	151.6	−82
75% Percentile (Q3)	77.9	13.2	170.3	−118.5
IQR	22.1	12.2	78.3	−57.7
Mean ± SD	70.5 ± 11	9.9 ± 8.5	146.3 ± 25.2	−79.7 ± 25.1

Abbreviations: HR, heart rate; bpm, beats per minute; SBP, systolic blood pressure; mmHg, millimeters of mercury; IQR interquartile range; SD, standard deviation.

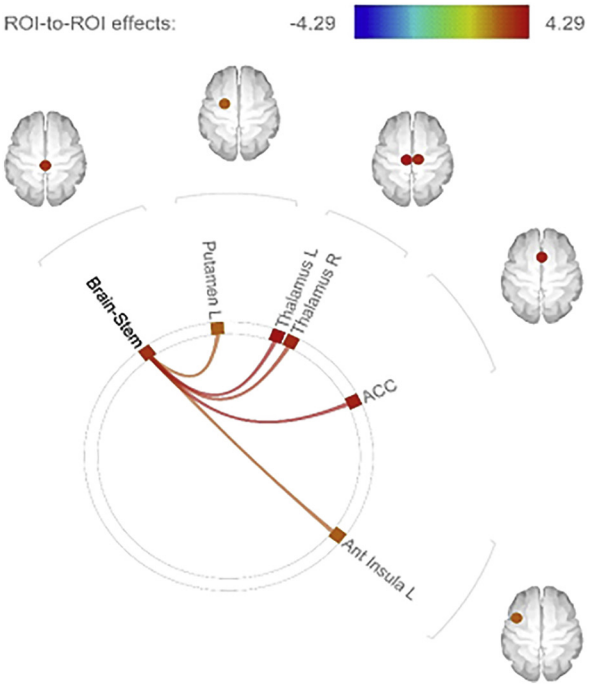

Brainstem Target	Effect Size
(L) Putamen	0.26
(L) Thalamus	0.41
(R) Thalamus	0.34
ACC	0.36
(L) Ant. Insula	0.26

Fig. 1. Brainstem functional connecitivity at rest [controls > patients]. At rest, controls had significantly greater brainstem connectivity compared to NOH patients. Strength of connectivity is represented across a colour spectrum with red representing larger T-values and stronger connectivity. Abbrev. L/R, left/right; ACC, anterior cingulate cortex; Ant, anterior; Thal, Thalamus; ROI, region of interest.

resolution 1.0 × 1.0 × 1.0 mm, 1 mm slice thickness, no gap, flip angle 9°, TE: 2.98 ms, TI: 900 ms, TR: 2300 ms). Blood oxygen level-dependent (BOLD) signals were acquired using a T2- weighted gradient echo-echo planar imaging pulse sequence with the following parameters: TE: 30 ms; FOV: 240 × 240mm; flip angle: 40°; multiband acceleration factor: 4. Forty-eight interleaved axial slices (3.0 × 3.0 mm in-plane voxel resolution, TR: 1000 ms) were acquired in each volume. To help minimize head movement each participant's head was placed in a head cradle packed with foam padding.

2.3. Neuroimaging protocol

Participant completed 5 min of rest followed by three Valsalva maneuvers (VM) during a functional scan of their brain. Rest: For all participants, the resting period consisted of 5 min during which, all participants were instructed to remain still with their eyes closed, but not to fall asleep. Valsalva maneuver: The Valsalva session was modeled as a blocked design switching between periods of rest and the maneuver. Following a 1-min baseline, participants were instructed to take a deep breath in, followed immediately by an exhalation to be maintained at an expiratory pressure of 40 mmHg, held for 15-s. The maneuver was repeated three times separated by a 2-min (120 s) rest in between trials. The first 10 s immediately following release of the maneuver was recorded as a recovery period. The remaining 110 s were recorded as a rest period to allow for hemodynamics to return to baseline prior to performing another Valsalva. Together, the Valsalva scanning duration was 465 s (7 min, 45 s). All participants were provided real-time visual feedback of their expiratory pressure to ensure the maneuver was performed correctly. To further minimize head movement during VM, all participants practiced the maneuver prior to scanning while being supervised. In addition, during the scanning session, an MRI technician provided feedback if there was excessive movement, in which case the maneuvers were repeated. Beat-to-beat heart rate was recorded from a continuous signal derived from an MRI-compatible pulse oximeter (Nonin Medical, 8600FO MRI, Plymouth, MN). All hemodynamic recordings were collected using WR TestWorks™ software (WR Medical Electronics Co., Stillwater, MN).

2.4. Neuroimaging analysis

All imaging data were analyzed using the Conn functional connectivity toolbox (v18a) available through SPM12 (Wellcome Department of Imaging Neuroscience, London, UK) using a MATLAB R2016b interface (Mathworks, Natick, MA). Preprocessing steps included realignment, unwarping and slice-time correction. All structural and functional images were segmented in grey matter, white matter and cerebral spinal fluid, normalized to Montreal Neurological Institute (MNI) space and smoothed with a Gaussian kernel (Full-Width Half-Max = 6 mm). In addition to realignment, the ART-based scrubbing method was further used to detect outlier volumes with high motion (ART parameters: 2-mm subject motion threshold and a global signal threshold set at Z = 9). Nuisance variables including: 6 realignment parameters, first 5 principle components from the white matter and CSF and the outlier volumes from the scrubbing procedure were then regressed out of the signal. The data were linearly detrended and a band-pass filter of 0.008 to 0.09 Hz was applied. A brainstem mask was used as the brainstem seed source, and all areas for connectivity were defined on an ROI basis using an ROI-to ROI approach at rest and during Valsalva maneuver. Cortical (91 ROIs) and subcortical (15 ROIs) atlases from the Harvard-Oxford Atlas and cerebellum parcellation (26 ROIs) atlas from AAL atlas were used in the ROI analysis. In the first level analysis, ROI-to-ROI maps were generated for each individual during the predefined conditions. Individual connectivity maps were created using the General Linear Model convolved with a canonical hemodynamic response function. In the second-level analysis, a between-subjects contrast (controls > patients [1, −1]; patients > controls [−1, 1]) was performed on the basis of a random-effects general linear model, with a seed-level correction for multiple comparisons (false-discovery rate: $p < .05$).

3. Results

3.1. ROI-to-ROI functional connectivity

Rest: Compared to NOH patients, at rest controls had significantly greater brainstem connectivity to the anterior cingulate cortex (ACC) (T-value: 4.29; p-FDR < 0.001), left anterior insula (T-value: 3.31; p-

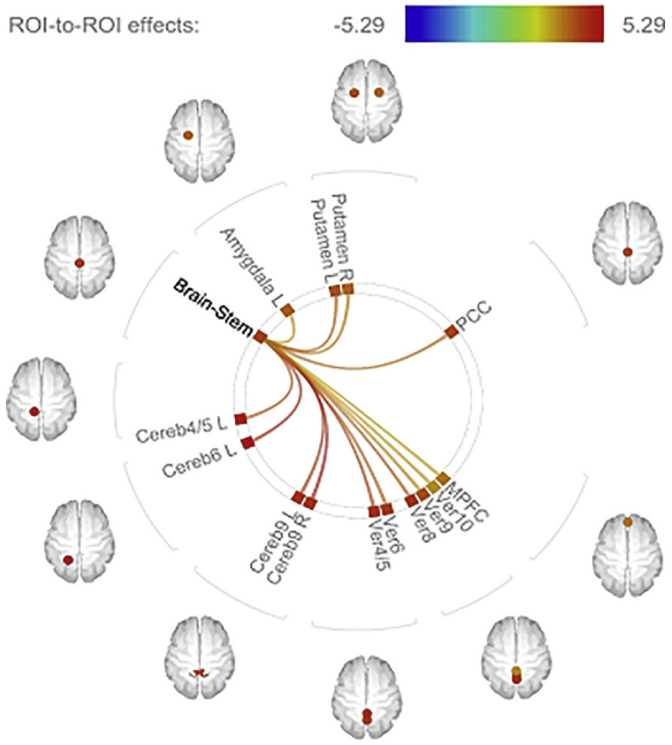

Fig. 2. Brainstem functional connecitivity during Valsalva maneuver [controls > patients]. During Valsalva maneuver, controls had significantly more brainstem connectivity to the amygdala, bilateral putamen, PCC, MPFC and cerebellum compared to NOH patients. Strength of connectivity is represented across a colour spectrum with red representing larger T-values and stronger connectivity. Abbrev. L/R, left/right; PCC, posterior cingulate cortex; ROI, region of interest; MPFC, medial prefrontal cortex.

FDR < 0.001), left putamen (T-value: 3.31; p-FDR < 0.005) and bilateral thalamus (T_R-value: 3.83; T_L-value: 4.25; p-FDR < 0.001) (Fig. 1). The effect sizes for the aforementioned brainstem-to-ROI connectivities ranged from small to moderate (Fig. 1).

Valsalva (VM): During VM, controls also showed significantly more connectivity between the brainstem and both the left anterior (cerebellum 4/5) and bilateral posterior cerebellum (cerebellar 9 and left cerebellar 6). Other cerebellar regions included brainstem-to-vermis (Vermis 4/5, 6, 8, 9 and 10). Other brainstem-to-cortical and subcortical regions included: bilateral putamen, posterior cingulate cortex, amygdala and medial prefrontal cortex (Fig. 2). The effect sizes were moderate-to-strong for each brainstem-to-ROI (Table 2). Moreover, there was a significant negative correlation between the brainstem-cerebellar connectivity and the total CASS (Table 3).

Valsalva recovery: During the recovery phase of the VM, controls had greater brainstem connectivity to the left thalamus (4.17; p-FDR = 0.02); PCC (3.32; p-FDR < 0.05); right putamen (3.28; p-FDR < 0.05); right paracingulate gyrus (3.25; p-FDR < 0.05) and left posterior cerebellum (C9: 3.21; p-FDR < 0.05). Similar to VM, the effect sizes for each brainstem-to-ROI was moderate-strong (Fig. 3).

4. Discussion

In the current study we compared functional connectivity measures between autonomic failure patients and age-matched controls at rest and during an autonomic challenge. Using the brainstem as a seed source we found the following significant findings: 1) Patients with autonomic failure showed significantly less brainstem connectivity to structures of the central autonomic network throughout a state of rest and in response to a Valsalva maneuver. 2) Brainstem-to-cerebellum connectivity was negatively correlated with the total CASS suggesting

Table 2
Targets with greater brainstem functional connectivity during VM in healthy controls.

Brainstem target	Side	T-value	P-FDR corrected	Effect size
Cerebellum 9	R	5.29	< 0.005	0.75
Cerebellum 6	L	4.82	< 0.005	0.90
Cerebellum 9	L	4.53	< 0.005	0.74
Vermis 4/5		4.31	< 0.01	0.76
Cerebellum 4/5	L	3.97	< 0.01	0.82
Vermis 6		3.88	< 0.01	0.72
Vermis 8		3.86	< 0.01	0.74
Putamen	L	3.78	< 0.01	0.63
PCC		3.70	< 0.01	0.68
Putamen	R	3.42	< 0.01	0.59
Vermis 9		3.15	< 0.05	0.64
Vermis 10		2.95	< 0.05	0.47
Amygdala	L	2.91	< 0.05	0.60
MPFC		2.82	< 0.05	0.54

Abbrev. VM, Valsalva maneuver; L/R, left/right; PCC, posterior cingulate cortex.

individuals with more severe and widespread autonomic dysfunction have reduced brainstem-cerebellar connectivity.

The cortical and subcortical structures found functionally linked to the brainstem represent well recognized findings from neuroimaging and autonomic literature. In the current study, patients had significantly less brainstem connectivity to key autonomic structures including the cerebellum, thalamus, cingulate cortices, medial prefrontal and insula. These regions have all been highly implicated in autonomic regulation both in animals and humans, and in health and disease (Shoemaker et al., 2015; Shoemaker and Goswami, 2015). The thalamus plays a pivotal role as the primary relay site for information and has an abundance of anatomical projections to cortical, subcortical and brainstem structures (Cechetto and Shoemaker, 2009; Shoemaker and Goswami, 2015). Moreover, both the posterior and anterior cingulate cortices are key contributors to autonomic regulation, specifically modulations of heart rate and blood pressure (Critchley, 2003; King et al., 1999; Shoemaker et al., 2015). For example, the anterior cingulate is commonly activated during maneuvers that elicit an increase in sympathetic activity such as the Valsalva maneuver, maximal inspiratory apneas and lower-body negative pressure. Furthermore, increased ACC activation has also been coupled with direct recordings of sympathetic nerve activity (Henderson et al., 2012). This is important, as improper regulation of heart rate, blood pressure and efferent sympathetic activity are cardinal features of autonomic failure. Moreover, the insula cortex (IC) has been highly investigated in autonomic regulation. Anatomically, the insula is reciprocally linked to brainstem autonomic nuclei (Dampney, 1994; Verberne et al., 1997), which provides an anatomical basis for autonomic influence. Functionally, the IC is extremely complicated. The IC has been partitioned into anterior/posterior portions as well as lateralized into left and right, each contributing separately to autonomic regulation. For example, stimulation of the rostral posterior IC in rats induced tachycardia while bradycardia was elicited via caudal stimulation (Oppenheimer and Cechetto, 1990). Furthermore, Zhang et al. (1998) demonstrated that damage to the left IC increased cardiac baroreceptor gain with no effect on heart rate or blood pressure, while right IC lesions resulted in increased baseline heart rate and blood pressure with no effect on gain (Zhang et al., 1998). Despite the complicated nature of the IC it is nevertheless involved in autonomic regulation. Finally, the current results extend beyond functional imaging studies, and coincides with existing functional connectivity literature in healthy controls, which also report significant brainstem connectivity with the ACC, thalamus, putamen and cerebellum (Bär et al., 2016).

A second key finding highlighted significantly less functional connectivity between the brainstem and the cerebellum/vermis during VM

Table 3
Brainstem-cerebellar connectivity during VM correlates negatively with total CASS.

	C9-R	C9-L	C6-L	C4/5-L	V4/5	V6	V8	V9	V10
Total CASS*	−0.725	−0.674	−0.738	−0.592	−0.626	−0.559	−0.589	−0.529	−0.594
P-value	< 0.001	=0.001	< 0.001	=0.006	=0.003	=0.01	=0.006	=0.016	=0.006

Abbrev: VM, Valsalva maneuver; CASS, composite autonomic scoring scale; C, Cerebellum; V, Vermis.
* Values represent r values.

in autonomic failure patients. The cerebellum is a cortical structure that is commonly seen in functional imaging studies particularly studies involving blood pressure perturbations. Moreover, there is a growing amount of evidence to support a key role for the cerebellum in regulating blood pressure and limiting blood pressure extremes (Holmes et al., 2002; Lutherer et al., 1983). Therefore, the cerebellum may play a key role during the VM where there are large blood pressure fluctuations, and absent compensatory responses in autonomic failure. For example, patients demonstrate large blood pressure reductions during early phase II of the maneuver without an appropriate sympathetically mediated late phase II response. Similarly, following release of the maneuver, an additional burst of sympathetic activation acts to increase blood pressure back to, or above baseline levels – a response that is also absent in autonomic failure. Both responses require increased sympathetic activation to alter blood pressure and this becomes important as the cerebellum is involved, in part, with sympathetic activation through direct projections with brainstem nuclei, including the NTS and RVLM (Paton and Spyer, 1990; Silva-Carvalho et al., 1991). Evidence of reduced brainstem connectivity to the cingulate, insula and cerebellum coincide with imaging studies with concurrent recordings of sympathetic nerve activity that have correlated these regions to increased sympathetic activity (Henderson et al., 2012).

Despite a patient population consisting of autonomic failure involving post-ganglionic impairment, the current results also suggest impaired functional connectivity between the brainstem and autonomic brain structures. Recent advances in network sensitive neuroimaging techniques have begun to identify distinct patterns of functional connectivity in various diseases (Buckner et al., 2009; Seeley et al., 2009). As a result, various hypotheses have emerged to explain the role neuronal networks may play in clinical progression of various diseases. Two disease-mechanism models have been hypothesized, which may help explain the current results: 1. The Nodal stress model, and 2. Transneuronal spread. The nodal stress model postulates that certain regions, or "nodes" within the brain that are subject to heavy network trafficking may be more vulnerable to activity-related "wear and tear"(Buckner et al., 2009; Saxena and Caroni, 2011). The brainstem is the primary site for afferent input and as such sends and receives afferent information on a continuous basis to ensure proper neurovascular function. In addition to afferent feedback, efferent signals from higher cortical and sub-cortical structures also contribute to proper autonomic regulation through direct and indirect projections to the brainstem (Cechetto and Shoemaker, 2009). Together the brainstem is a critical hub for autonomic inputs, and the abundance of intra-network information may influence regional neurodegeneration that is activity-dependent. In a disease that fails to properly regulate autonomic responses such as blood pressure, various afferent and efferent inputs may overload brainstem networks in an attempt to rectify the failed responses. However, even if the appropriate efferent signals can be sent, the post-ganglionic lesion would interrupt the signal leading to more feedback, ultimately resulting in a viscous cycle of chronic elevated activity and possibly an eventual pathological state.

The mechanism of transneuronal spread suggests that neurodegeneration between cortical networks progresses via axonal connections (Harris et al., 2010). Seeley et al., further suggest that disease progression starts at a primary network (i.e. the brainstem) and is more likely to extend into networks with stronger functional relationships (Seeley et al., 2008). This is important for two primary reasons. First, the results demonstrate that the cortical regions that showed significant differences between patients and controls were structures of the central autonomic network, and would therefore have a strong functional and

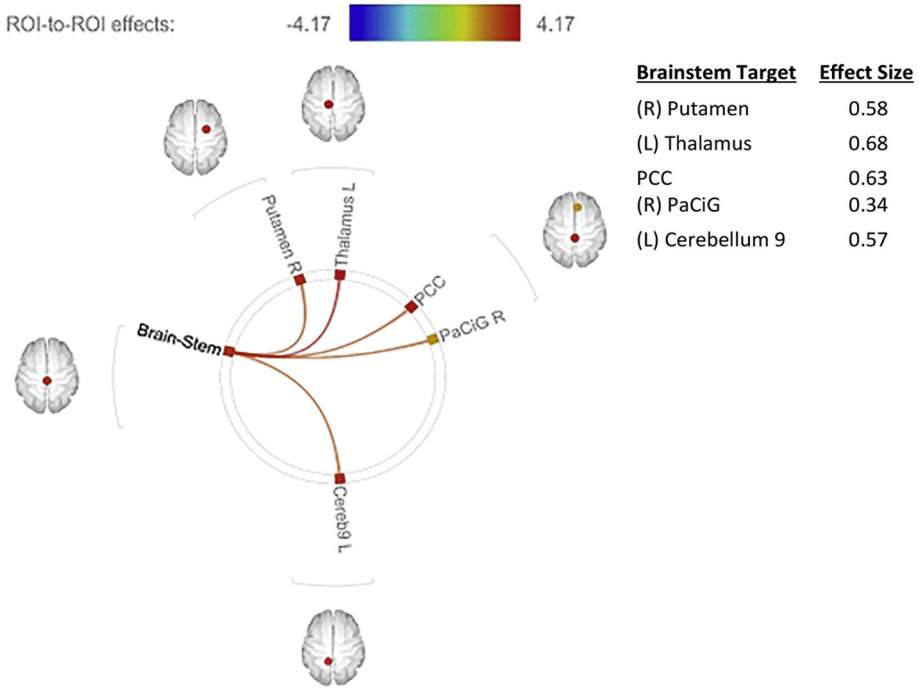

Fig. 3. Brainstem functional connecitivity during recovery phase of Valsalva maneuver [controls > patients]. Controls had significantly more brainstem functional connectivity during the recovery phase of Valsalva. Strength of connectivity is represented across a colour spectrum with red representing larger T-values and stronger connectivity. Abbrev. L/R, left/right; PaCig, paracingulate gyrus; PCC, posterior cingulate cortex; ROI, region of interest.

structural relationship with the brainstem. Second, this model predicts that networks with shorter functional paths to the epicenter will be more vulnerable once the disease is present (Zhou et al., 2012). Anatomically speaking, the cerebellum not only has direct projections with the brainstem but also demonstrates a relatively short functional pathway, and the strength of the brainstem-cerebellum connectivity was negatively correlated with autonomic severity and distribution.

4.1. Clinical implications

The following findings may provide insight into differential susceptibility to patient fall risk, increased morbidity and/or more severe autonomic dysfunction. This hypothesis is congruent with the results of Zhou et al., (2012) who applied functional connectivity in healthy controls to provide new insights into how the brain's functional connectivity may predict vulnerability to neurodegenerative disease (Zhou et al., 2012).

Cerebellar impairment and/or reduced cerebellar-brainstem connectivity may contribute/worsen common symptomatology seen with NOH patients including postural light-headedness and dizziness. Light-headedness and dizziness are the primary cause of morbidity in patients with autonomic failure, which have the potential to be exacerbated by cerebellar dysfunction. For example, similar to postural symptomatology commonly seen with autonomic dysfunction, cerebellar dizziness induced by a change in position from sitting to standing, has also been reported in posterior cerebellar and vermis lesions (Bodranghien et al., 2016). Furthermore, following an acute cerebellar infarct, one study found that 28% of patients developed postural dizziness on standing and 31% showed evidence of adrenergic dysfunction characterized by orthostatic hypotension and absent adrenergic phases in response to Valsalva maneuver (Kim and Lee, 2016). Therefore, reduced cerebellar-brainstem connectivity may not only worsen postural symptoms, but also contribute further to adrenergic failure and autonomic dysfunction. Together these two outcomes would increase patient morbidity, increase susceptibility to fall related injuries and reduce a patient's ability to live independently.

4.2. Study limitations

Despite the promising contributions that these data may add to our understanding of autonomic failure, the current study contains the following limitations. 1) The current study applied a brainstem mask that covered the whole brainstem. Certainly, there are a number of brainstem nuclei that have different contributions to autonomic control. In the current study, we did not focus on whether the brainstem shows increased or decreased activity, simply that there was reduced connectivity to key cortical and subcortical sites. The authors believe the next logical step will be to assess functional connectivity related to specific brainstem nuclei. 2) The two proposed mechanistic models have been primarily investigated in neurodegenerative disorder such as Alzheimer's Disease, PD, Huntington's disease and Amyotrophic Lateral Sclerosis. Even though there are neurodegenerative diseases associated with autonomic failure, this work has yet to include these patient populations. Further studies are needed to investigate these models in autonomic failure. 3) Blood pressure data was not directly measured during the MRI session as this often involves the invasive insertion of an arterial line. Therefore, in the current study the heart rate change during the MRI session was compared with the heart rate changes that occurred in the laboratory during the Valsalva maneuver. Additionally, the expiratory pressure during the maneuver was monitored to ensure compliance. If there was a similar heart rate response, it was assumed that the corresponding blood pressure changes in response to the maneuver were similar. 4) The current study had a heterogeneous patient population, including patients diagnosed with PD plus autonomic failure. To test whether the current results were related to autonomic failure and not PD, a sub-analysis of the patient population was performed. No significant differences between our autonomic failure patients with and without PD were found, suggesting the current results are related to the presence of autonomic failure and not PD pathology.

5. Conclusion

In the current study, patients with peripheral autonomic failure had significantly less functional connectivity between the brainstem and key cortical autonomic structures both at rest and during an autonomic maneuver. Patients showed reduced coupling between brainstem and regions of the central autonomic network, including the cerebellum, insula, thalamus and cingulate cortices. These results may be attributed to two mechanistic models, including nodal stress and transneuronal spread, which may contribute, in part, to the pathophysiology of autonomic failure.

Acknowledgements

This work was partly funded by the Canada First Research Excellence Fund, to BrainsCAN, Canada. The authors would also like to thank Scott Charlton for his excellent technical services during MRI data collection.

References

Baker, J., Paturel, J.R., Kimpinski, K., 2018. Impaired cortical autonomic responses during sympathetic activation in neurogenic orthostatic hypotension characterized by postganglionic autonomic dysfunction. J. Appl. Physiol. 125, 1210–1217.
Baker, J., Paturel, J.R., Kimpinski, K., 2019. Cerebellar impairment during an orthostatic challenge in patients with neurogenic orthostatic hypotension. Clin. Neurophysiol. 130, 189–195.
Bär, K.-J., De La Cruz, F., Schumann, A., Koehler, S., Sauer, H., Critchley, H., Wagner, G., 2016. Functional connectivity and network analysis of midbrain and brainstem nuclei. Neuroimage 134, 53–63.
Benarroch, E.E., 1993. The central autonomic network: functional organization, dysfunction, and perspective. Mayo Clin. Proc. 68, 988–1001.
Bodranghien, F., Bastian, A., Casali, C., Hallett, M., Louis, E., Manto, M., Marien, P., Nowark, D., Schmahmann, J., Serrao, M., Steiner, K., Strupp, M., Tilikete, C., Timmann, D., van Dun, K., 2016. Consensus paper: revisiting the symptoms and signs of cerebellar syndrome. Cerebellum 15, 369–391.
Buckner, R.L., Sepulcre, J., Talukdar, T., Krienen, F., Liu, H., Hedden, T., Andrews-Hanna, J.R., Sperling, R.A., Johnson, K.A., 2009. Cortical hubs revealed by intrinsic functional connectivity: mapping, assessment of stability, and relation to Alzheimer's disease. J. Neurosci. 29, 1860–1873.
Castle, M., Comoli, E., Loewy, A.D., 2005. Autonomic brainstem nuclei are linked to the hippocampus. Neuroscience 134, 657–669.
Cechetto, D.F., Shoemaker, J.K., 2009. Functional neuroanatomy of autonomic regulation. Neuroimage 47, 795–803.
Critchley, H.D., 2003. Human cingulate cortex and autonomic control: converging neuroimaging and clinical evidence. Brain 126, 2139–2152.
Dampney, R.A.L., 1994. Functional organization of central pathways regulating the cardiovascular system. Physiol. Rev. 74, 323–364.
Gibbons, C.H., Freeman, R., Kaufmann, H., 2017. The recommendations of a consensus panel for the screening, diagnosis, and treatment of neurogenic orthostatic hypotension and associated supine hypertension. J. Neurol. 264, 1567–1582.
Harris, J.A., Devidze, N., Verret, L., Ho, K., Halabisky, B., Thwin, M.T., Kim, D., Hamto, P., Lo, I., Yu, G.-Q., Palop, J.J., Masliah, E., Mucke, L., 2010. Transsynaptic progression of amyloid-β-induced neuronal dysfunction within the entorhinal-hippocampal network. Neuron 68, 428–441.
Henderson, L.A., James, C., Macefield, V.G., 2012. Identification of sites of sympathetic outflow during concurrent recordings of sympathetic nerve activity and fMRI. Anat. Rec. 295, 1396–1403.
Holmes, M.J., Cotter, L.A., Arendt, H.E., Cass, S.P., Yates, B.J., 2002. Effects of lesions of the caudal cerebellar vermis on cardiovascular regulation in awake cats. Brain Res. 938, 62–72.
Kim, H.-A., Lee, H., 2016. Orthostatic hypotension in acute cerebellar infarction. J. Neurol. 263, 120–126.
King, A.B., Menon, R.S., Hachinski, V., Cechetto, D.F., 1999. Human forebrain activation by visceral stimuli. J. Comp. Neurol. 413, 572–582.
Low, P., 1993. Composite autonomic scoring scale for laboratory quantification of generalized autonomic failure. Mayo Clin. Proc. 68, 748–752.
Lutherer, L., Lutherer, B., Dormer, K., Janssen, H., Barnes, C., 1983. Bilateral lesions of the fastigial nucleus pervents the recovery of blood pressure following hypotension induced by hemorrhage or administration of endotoxin. Brain Res. 269, 251–257.
Oppenheimer, S.M., Cechetto, D.F., 1990. Cardiac chronotropic organization of the rat insular cortex. Brain Res. 533, 66–72.
Oppenheimer, S.M., Gelb, A., Girvin, J., Hachinski, V., 1992. Cardiovascular effects of human insular cortex stimulation. Neurology 42, 1727–1732.

Paton, J.F.R., Spyer, K.M., 1990. Brain stem regions mediating the cardiovascular responses elicited from the posterior cerebellar cortex in the rabbit. J. Physiol. 427, 533–552.
Saper, C.B., 1982. Reciprocal parabrachial-cortical connections in the rat. Brain Res. 242, 33–40.
Saxena, S., Caroni, P., 2011. Review selective neuronal vulnerability in neurodegenerative diseases: from stressor thresholds to degeneration. Neuron 71, 35–48.
Seeley, W.W., Crawford, R., Rascovsky, K., Kramer, J.H., Weiner, M., Miller, B.L., Gorno-Tempini, M.L., 2008. Frontal paralimbic network atrophy in very mild behavioral variant frontotemporal dementia. Arch. Neurol. 65, 249–255.
Seeley, W.W., Crawford, R.K., Zhou, J., Miller, B.L., Greicius, M.D., 2009. Neurodegenerative diseases target large-scale human brain networks. Neuron 62, 42–52.
Shoemaker, J.K., Goswami, R., 2015. Forebrain neurocircuitry associated with human reflex cardiovascular control. Front. Physiol. 6, 1–14.
Shoemaker, J.K., Norton, K.N., Baker, J., Luchyshyn, T., 2015. Forebrain organization for autonomic cardiovascular control. Auton. Neurosci. Basic Clin. 188, 5–9.
Silva-Carvalho, L., Paton, J.F.R., Goldsmith, G.E., Spyer, K.M., Spyer, K.M., 1991. The effects of electrical stimulation of lobule IXb of the posterior cerebellar vermis on neurones within the rostral ventrolateral medulla in the anaesthetised cat. J. Auton. Nerv. Syst. 36, 97–106.
Verberne, A.J., Owens, N.C., 1998. Cortical modulation of the cardiovascular system. Prog. Neurobiol. 54, 149–168.
Verberne, A.J.M., Lam, W., Owens, N.C., Sartor, D., 1997. Supramedullary modulation of sympathetic vasomotor function. Clin. Exp. Pharmacol. Physiol. 24, 748–754.
Zhang, Z.H., Rashba, S., Oppenheimer, S.M., 1998. Insular cortex lesions alter baroreceptor sensitivity in the urethane-anesthetized rat. Brain Res. 813, 73–81.
Zhou, J., Gennatas, E.D., Kramer, J.H., Miller, B.L., Seeley, W.W., 2012. Predicting regional neurodegeneration from the healthy brain functional connectome. Neuron 73, 1216–1227.